2020 International Symposium on Power Electronics,
Electrical Drives, Automation and Motion

Optimal Multi-Harmonic Current Injection Strategy for an Asymmetrical Nine-Phase PMSM

A. Cervone[1], *Student Member*, *IEEE*, M. Slunjski[2], *Student Member*, *IEEE*, E. Levi[2], *Fellow, IEEE*, G. Brando[1]
[1] Dept. of Electrical Engineering, University of Naples Federico II, 80125, Naples, Italy
[2] Faculty of Engineering and Technology, Liverpool John Moores University, Liverpool L3 3AF, U.K.

***Abstract* — The paper develops a strategy to enhance the torque development for a nine-phase PMSM with an asymmetrical winding configuration and a single isolated neutral point. The approach is based on the simultaneous exploitation of different spatial harmonics of the magnetic flux density in the air-gap, which requires both a non-sinusoidal set of PM induced back-EMFs and a non-sinusoidal set of phase currents (thus implying the injection of multiple harmonics). By formulating the machine's mathematical model in a proper multiple synchronous reference frames, the electromagnetic torque is given by the superposition of different harmonic quadrature current component contributions: their simultaneous utilization allows to meet a set optimization goal. The proposed approach focuses on the minimization of the average stator losses for a given reference torque. The optimal solution is found analytically and validated numerically for a specific case study. With respect to the sole fundamental current exploitation, the proposed technique allows for a significant reduction of the average losses but, given the machine's configuration, it requires an uneven distribution of the third harmonic current component among the nine phases.**

Keywords* — *Multiphase drives, surface mounted PMSM, asymmetrical winding, nine-phase, non-sinusoidal back-EMF, harmonic current injection, power loss minimization.

I. INTRODUCTION

In the recent years, multiphase electric drives have become interesting solutions both for industrial and traction applications. Indeed, they have been identified as promising systems in many fields, including wind turbine plants, terrestrial (cars and trains), marine and aerospace vehicles. When compared to the three-phase counterparts, multiphase configurations show several advantages, such as reduced phase currents (at equal power levels), higher fault tolerance, higher efficiency (at least in theory) and higher torque density [1-3].

One of the advantages of multiphase machine is the possibility to enhance the torque development through a proper harmonic injection into the phase currents [4-7]. Indeed, the different harmonic currents can be controlled to properly shape the magnetic flux density in the machine's air-gap. When the field is non-sinusoidal, it can be equivalently represented as the superposition of several spatial harmonics, each of which can actively contribute to the overall torque development. The system then presents several degrees of freedom and allows for the optimization of the machine performances, like the minimization of the power losses.

For permanent magnet synchronous machines (PMSMs) the torque improvement through the exploitation of higher order spatial harmonics can be achieved once the back-EMFs induced by the permanent magnets (PMs) are non-sinusoidal functions of the rotor's electrical position.

The simultaneous exploitation of the fundamental current component and of an additional third harmonic injection has been widely covered in the technical literature, especially for five-phase machines [8-16]. A third harmonic injection strategy has been presented in [17] for a symmetrical nine-phase PMSM.

On the other hand, only few examples have been proposed for the torque enhancement in asymmetrical configurations, and most of these works focus on asymmetrical six-phase machine [18-20]. In such cases, it has been shown that the torque enhancement via a third harmonic injection requires a zero-sequence current path, which can be obtained by connecting the machine's neutral point to either an additional inverter leg or to the midpoint of the capacitor bank in the inverter's dc link [18-19].

The simultaneous utilization of multiple harmonics in multiphase PMSMs has been investigated to a far less extent. An example can be found in [20], where a simultaneous fifth and seventh harmonic current injection has been exploited to enhance the torque developed by the fundamental current contribution while respecting a maximum peak phase current constraint.

It has been shown in [21-22] that, even in the absence of a neutral connection path, the third harmonic injection can be exploited for the torque enhancement in an asymmetrical nine-phase PMSM: the optimal injection ratio has been found with the aim to minimize the average stator power losses for a given reference torque, while the zero-sequence current constraint has been met by unevenly distributing the third harmonic current among the phases. This paper extends the results obtained in [21], by formulating a strategy to exploit multiple harmonics injection for the same asymmetrical nine-phase machine configuration. The problem is formalized by studying the machine's mathematical model in the multiple synchronous reference frames and solved analytically with respect to the PMs' induced flux parameters. The proposed approach has been numerically validated and compared with the fundamental harmonic exploitation only, and with the optimal third harmonic injection strategy discussed in [21]. The results show that a significant decrease of the average power losses can be achieved by using all the quadrature current components in the multiple synchronous reference frames, which leads to an optimal injection of all odd order harmonics up to the 7th into the machine's phase currents.

The paper is structured as follows. Section II recalls the machine's mathematical model in both the phase variables domain and the multiple synchronous reference frames. Then, Section III formulates the power loss minimization problem and develops its analytical solution. Section IV particularizes the proposed approach for a specific nine-phase case study and shows the numerical results. Finally, Section V summarises the conclusions of the paper.

978-1-7281-7019-0/20/$31.00 ©2020 IEEE

II. Mathematical Model

The mathematical model of the asymmetrical nine-phase PMSM under analysis has been presented in [21-22] and is briefly recalled in the present section.

The nine stator windings (which are identified by the index $k = 1, \ldots, 9$) are grouped in three symmetrical three-phase sets (referred to as $\{a_1,b_1,c_1\}$, $\{a_2,b_2,c_2\}$ and $\{a_3,b_3,c_3\}$); with respect to the machine's electrical angles (related to the P_p pole pairs), the windings of each set are mutually shifted by 120°, while the different sets are shifted by 20° one from the other. The magnetic axes configuration is synthetically represented by the angle set (Fig. 1a):

$$[\alpha] = [0° \; 120° \; 240° \,|\, 20° \; 140° \; 260° \,|\, 40° \; 160° \; 280°] \tag{1}$$

As represented in Fig. 1b, the machine's windings are star-connected with a single isolated neutral point and are supplied by a voltage source inverter (VSI).

A. Model in the Phase Variables Domain

The system model in terms of phase variables is:

$$\begin{cases} [u_{\text{ph}}] + v_{ON} \cdot [1_{9\times1}] = [v_{\text{ph}}] = R \cdot [i_{\text{ph}}] + [L] \cdot \dfrac{\text{d}}{\text{d}t}[i_{\text{ph}}] + [e_{\text{ph}}] \\ [1_{1\times9}] \cdot [i_{\text{ph}}] = \sum_{k=1}^{9} i_k = 0 \\ T_{em} = P_p \cdot [i_{\text{ph}}]^{\text{T}} \cdot \dfrac{\partial}{\partial\theta}[\lambda_{\text{ph}}] = P_p \cdot \sum_{k=1}^{9} i_k \cdot \dfrac{\partial \lambda_k}{\partial\theta} \\ p = R \cdot [i_{\text{ph}}]^{\text{T}} \cdot [i_{\text{ph}}] = \sum_{k=1}^{9} R \cdot i_k^2 \end{cases} \tag{2}$$

where:

- $[u_{\text{ph}}]$ is the set of the inverter's leg voltages,
- v_{ON} is the voltage between the inverter's dc-bus mid-point O and the machine's neutral point N,
- $[v_{\text{ph}}]$ is the set of the stator winding voltages,
- $[i_{\text{ph}}]$ is the set of the stator winding currents,
- $[\lambda_{\text{ph}}]$ is the set of the PM induced fluxes,
- $[e_{\text{ph}}] = \text{d}[\lambda_{\text{ph}}]/\text{d}t$ is the set of the PM induced back-EMFs,
- $[L]$ is the stator winding inductance matrix (which includes both the mutual and the leakage contributions),
- R is the equivalent stator winding resistance,
- T_{em} is the developed electromagnetic torque,
- θ is the electric angle between the rotor reference axis and the stator reference one, and
- p is the total stator winding power dissipation.

The non-sinusoidal flux density and field in the machine's air-gap affect the PM's induced fluxes, which are hence themselves non-sinusoidal functions of the rotor's electrical position θ. By only considering the odd-order harmonics up to the 7-th, the k-th phase induced flux can be expressed as:

$$\begin{aligned} \lambda_k(\theta) &= \lambda_{M1}\cos(\theta - \alpha_k) + \lambda_{M3}\cos\big(3(\theta - \alpha_k) + \varphi_3\big) + \ldots \\ &\ldots + \lambda_{M5}\cos\big(5(\theta - \alpha_k) + \varphi_5\big) + \lambda_{M7}\cos\big(7(\theta - \alpha_k) + \varphi_7\big) \end{aligned} \tag{3}$$

where λ_{Mh} and φ_h are the magnitude and the phase displacement of the h-th spatial harmonic contribution.

B. Model in the Multiple Synchronous Domains

The nine-phase PMSM mathematical model (1) can be rewritten in multiple synchronous reference frames by applying the Vector Space Decomposition (VSD) and rotational transformation to each phase variable set $[f_{\text{ph}}] = [f_{a1},f_{b1},f_{c1},f_{a2},f_{b2},f_{c2},f_{a3},f_{b3},f_{c3}]^{\text{T}}$. The final current set $[f_{\text{dq}}] = [f_{\text{d1}},f_{\text{q1}},f_{\text{d3}},f_{\text{q3}},f_{\text{d5}},f_{\text{q5}},f_{\text{d7}},f_{\text{q7}},f_0]^{\text{T}}$ is a linear combination of the phase variables obtained by left-multiplying the vector $[f_{\text{ph}}]$ with the transformation matrices:

$$[\text{C}] = \sqrt{\frac{2}{9}} \cdot \begin{bmatrix} \cos([\alpha]) \\ \sin([\alpha]) \\ \cos(3\cdot[\alpha]) \\ \sin(3\cdot[\alpha]) \\ \cos(5\cdot[\alpha]) \\ \sin(5\cdot[\alpha]) \\ \cos(7\cdot[\alpha]) \\ \sin(7\cdot[\alpha]) \\ [1]^{\text{T}}/\sqrt{2} \end{bmatrix} \quad \begin{pmatrix} \text{with the inverse} \\ \text{being referred to} \\ \text{as } [\text{T}] = [\text{C}]^{-1} \end{pmatrix} \quad \text{and} \tag{4}$$

$$[\text{D}](\theta) = \begin{bmatrix} [\text{D}_1](\theta) & [0_{2\times2}] & [0_{2\times2}] & [0_{2\times2}] & [0_{2\times1}] \\ [0_{2\times2}] & [\text{D}_3](\theta) & [0_{2\times2}] & [0_{2\times2}] & [0_{2\times1}] \\ [0_{2\times2}] & [0_{2\times2}] & [\text{D}_5](\theta) & [0_{2\times2}] & [0_{2\times1}] \\ [0_{2\times2}] & [0_{2\times2}] & [0_{2\times2}] & [\text{D}_7](\theta) & [0_{2\times1}] \\ [0_{1\times2}] & [0_{1\times2}] & [0_{1\times2}] & [0_{1\times2}] & 1 \end{bmatrix} \tag{5}$$

$$\text{with} \quad [\text{D}_h](\theta) = \begin{bmatrix} \cos(h\theta + \varphi_h) & \sin(h\theta + \varphi_h) \\ -\sin(h\theta + \varphi_h) & \cos(h\theta + \varphi_h) \end{bmatrix}$$

As shown in [21-22], while the rotational matrix $[\text{D}]^{\text{T}}(\theta)$ is always unitary (i.e. $[\text{D}]^{-1}(\theta) = [\text{D}]^{\text{T}}(\theta)$), the generalized Clarke transformation matrix associated to the asymmetrical angle configuration (1) does not meet the orthogonality condition, meaning that $[\text{T}] = [\text{C}]^{-1} \neq [\text{C}]^{\text{T}}$.

The transformations between the two sets are given by:

$$[f_{\text{dq}}] = [\text{D}](\theta) \cdot [\text{C}] \cdot [f_{\text{ph}}] \;\Leftrightarrow\; [f_{\text{ph}}] = [\text{T}] \cdot [\text{D}]^{\text{T}}(\theta) \cdot [f_{\text{dq}}] \tag{6}$$

By applying (6) to the phase variable model (2) and by explicitly considering (3), the resulting model is written as:

$$\begin{cases} [u_{\text{dq}}] + v_{ON} \cdot [\text{g}](\theta) = [v_{\text{dq}}] = R \cdot [i_{\text{dq}}] + \ldots \\ \quad \ldots + [L_{\text{dq1}}](\theta) \cdot \dfrac{\text{d}}{\text{d}t}[i_{\text{dq}}] + \omega \cdot [L_{\text{dq2}}](\theta) \cdot [i_{\text{dq}}] + [e_{\text{dq}}] \\ i_0 = [0 \;\; 0 \;\; 0 \;\; 0 \;\; 0 \;\; 0 \;\; 0 \;\; 0 \;\; 1] \cdot [i_{\text{dq}}] = 0 \\ T_{em} = [\kappa]^{\text{T}} \cdot [i_{\text{dq}}] = \kappa_{\text{q1}} i_{\text{q1}} + \kappa_{\text{q3}} i_{\text{q3}} + \kappa_{\text{q5}} i_{\text{q5}} + \kappa_{\text{q7}} i_{\text{q7}} \\ p = R \cdot [i_{\text{dq}}]^{\text{T}} \cdot [\text{G}](\theta) \cdot [i_{\text{dq}}] \end{cases} \tag{7}$$

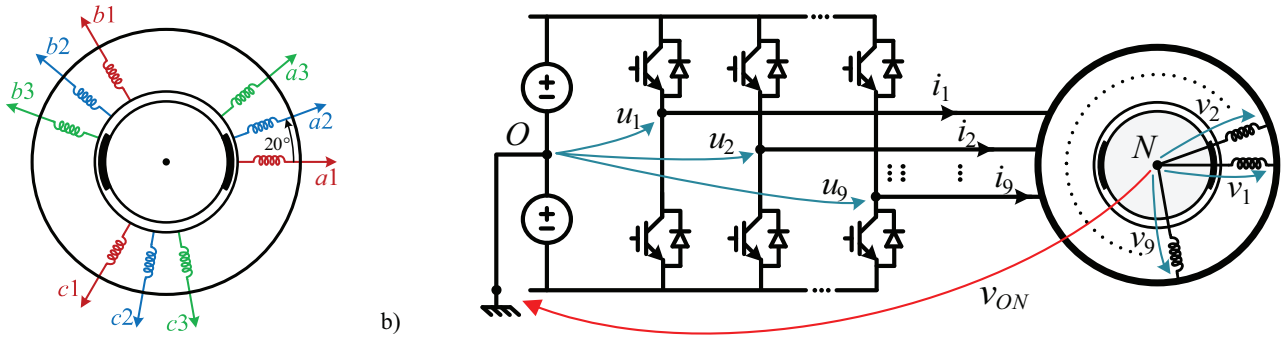

Fig. 1. Asymmetrical nine-phase PMSM under analysis: a) disposition of magnetic axes; b) system architecture.

where:

- $\omega = \mathrm{d}\theta/\mathrm{d}t$ is the rotor electrical angular speed,
- $[\mathrm{g}](\theta) = [\mathrm{D}](\theta)\cdot[\mathrm{C}]\cdot[1_{9\times1}]$ is a non-dimensional vector responsible for the coupling effects due to the neutral point potential shifting when $v_{ON} \neq 0$,
- $[L_{\mathrm{dq1}}](\theta) = [\mathrm{D}](\theta)\cdot[\mathrm{C}]\cdot[L]\cdot[\mathrm{T}]\cdot[\mathrm{D}]^{\mathrm{T}}(\theta)$ is the inductance matrix responsible for the transformer-induced back-EMFs,
- $[L_{\mathrm{dq2}}](\theta) = [\mathrm{D}](\theta)\cdot[\mathrm{C}]\cdot[L]\cdot[\mathrm{T}]\cdot\partial[\mathrm{D}]^{\mathrm{T}}(\theta)/\partial\theta$ is the inductance matrix responsible for the motional-induced back-EMFs,
- $[\kappa] = P_p\ \sqrt{9/2}\ [0\ \ \lambda_{M1}\ \ 0\ \ 3\lambda_{M3}\ \ 0\ \ 5\lambda_{M5}\ \ 0\ \ 7\lambda_{M7}\ \ 0]^{\mathrm{T}}$ is the equivalent torque gain vector, and
- $[\mathrm{G}](\theta) = [\mathrm{D}](\theta)\cdot[\mathrm{T}]^{\mathrm{T}}\cdot[\mathrm{T}]\cdot[\mathrm{D}]^{\mathrm{T}}(\theta)$ is a symmetric and positive definite matrix responsible for the non-uniform weighting of the different synchronous current components in the instantaneous power loss expression.

The average stator power losses can be found by averaging the instantaneous power p along a full rotor cycle. With a constant current set $[i_{\mathrm{dq}}]$, associated with multiple synchronous reference frames, one obtains:

$$\begin{aligned} P &= \frac{1}{2\pi}\int_0^{2\pi} p(\theta)\mathrm{d}\theta = \frac{1}{2\pi}\int_0^{2\pi} R\cdot[i_{\mathrm{dq}}]^{\mathrm{T}}\cdot[\mathrm{G}](\theta)\cdot[i_{\mathrm{dq}}]\mathrm{d}\theta = \\ &= R\cdot[i_{\mathrm{dq}}]^{\mathrm{T}}\cdot\left(\frac{1}{2\pi}\int_0^{2\pi}[\mathrm{G}](\theta)\mathrm{d}\theta\right)\cdot[i_{\mathrm{dq}}] = R\cdot[i_{\mathrm{dq}}]^{\mathrm{T}}\cdot[\mathrm{H}]\cdot[i_{\mathrm{dq}}] \end{aligned} \tag{8}$$

The matrix [H] identifies the weighting of each synchronous current component contribution in the average power losses. It can be analytically computed by averaging [G](θ) and it can be verified that it is a diagonal matrix:

$$[\mathrm{H}] = \frac{1}{2\pi}\int_0^{2\pi}[\mathrm{G}](\theta)\mathrm{d}\theta = \begin{bmatrix} 1 & 0 & 0 & 0 & 0 & 0 & 0 & 0 & 0 \\ 0 & 1 & 0 & 0 & 0 & 0 & 0 & 0 & 0 \\ 0 & 0 & 5 & 0 & 0 & 0 & 0 & 0 & 0 \\ 0 & 0 & 0 & 5 & 0 & 0 & 0 & 0 & 0 \\ 0 & 0 & 0 & 0 & 1 & 0 & 0 & 0 & 0 \\ 0 & 0 & 0 & 0 & 0 & 1 & 0 & 0 & 0 \\ 0 & 0 & 0 & 0 & 0 & 0 & 1 & 0 & 0 \\ 0 & 0 & 0 & 0 & 0 & 0 & 0 & 1 & 0 \\ 0 & 0 & 0 & 0 & 0 & 0 & 0 & 0 & 9 \end{bmatrix} \tag{9}$$

It can be noted that the (i_{d3}-i_{q3}) current components are weighted 5 times more than the other (i_{dh}-i_{qh}) components.

The chosen VSD and rotational transformation allow to simplify and to clearly highlight the influence of each synchronous current component on both the torque and the average power losses expressions. Nevertheless, given the asymmetrical windings configuration, the electrical equations show additional coupling effects which need to be properly compensated in the feedback current control [21-22]. It can be confirmed, using (7) that the 1st, 5th and 7th subspace equations take the standard decoupled form:

$$\begin{cases} u_{dh} = v_{dh} = Ri_{dh} + L_h\dfrac{\mathrm{d}i_{dh}}{\mathrm{d}t} - h\omega L_h i_{qh} \\ u_{qh} = v_{qh} = Ri_{qh} + L_h\dfrac{\mathrm{d}i_{qh}}{\mathrm{d}t} + h\omega L_h i_{dh} + e_{qh} \end{cases} \tag{10}$$

(with $h = 1,5,7$ and $e_{qh} = \sqrt{9/2}h\omega\lambda_{Mh}$). The 3rd subspace equations however depend on v_{ON} through the effect of [g](θ):

$$\begin{cases} u_{\mathrm{d3}} + 2\sqrt{2}\cos(3\theta+\varphi_3-\pi/3)v_{ON} = v_{\mathrm{d3}} = Ri_{\mathrm{d3}} + L_3\dfrac{\mathrm{d}i_{\mathrm{d3}}}{\mathrm{d}t} - 3\omega L_3 i_{\mathrm{q3}} \\ u_{\mathrm{q3}} + 2\sqrt{2}\cos(3\theta+\varphi_3+\pi/6)v_{ON} = v_{\mathrm{q3}} = Ri_{\mathrm{q3}} + L_3\dfrac{\mathrm{d}i_{\mathrm{q3}}}{\mathrm{d}t} + 3\omega L_3 i_{\mathrm{d3}} + e_{\mathrm{q3}} \end{cases} \tag{11}$$

(with $e_{\mathrm{q3}} = 9/\sqrt{2}\omega\lambda_{M3}$). The voltage v_{ON} is itself dependent on the (i_{d3}-i_{q3}) currents and the functional relationship can be explicitly found by considering the constraints $i_0 = 0$ (and $\mathrm{d}i_0/\mathrm{d}t = 0$) in the zero-sequence electrical equation of (7), resulting in:

$$\begin{cases} v_{ON} = \dfrac{L_{m3}}{9}\left[\left(2\sqrt{2}\sin(3\theta+\varphi_3+\pi/6)\right)\left(\dfrac{\mathrm{d}i_{\mathrm{d3}}}{\mathrm{d}t} - 3\omega i_{\mathrm{q3}}\right) + \ldots\right. \\ \left.\quad \ldots + \left(2\sqrt{2}\cos(3\theta+\varphi_3+\pi/6)\right)\left(\dfrac{\mathrm{d}i_{\mathrm{q3}}}{\mathrm{d}t} + 3\omega i_{\mathrm{d3}}\right)\right] + \dfrac{e_0 - u_0}{3} \end{cases} \tag{12}$$

(with $L_{m3} = L_3 - L_l$ and $e_0 = -6\omega\lambda_{M3}\sin(3\theta+\varphi_3-\pi/3)$).

III. Optimal Harmonic Injection Strategy

The standard Field Oriented Control (FOC) for surface mounted PMSMs controls only the i_{q1} current component of the $[i_{\mathrm{dq}}]$ set to achieve a desired reference torque T^*_{em}, while keeping all the other terms equal to zero. The resulting reference current is $i^*_{\mathrm{q1}} = T^*_{em}/\kappa_{\mathrm{q1}} = \sqrt{2/9}\cdot(T^*_{em}/P_p)\cdot(1/\lambda_{M1})$. Since $\mathrm{H}_{\mathrm{q1,q1}} = 1$, the corresponding average power losses are $P_{\mathrm{FUND}} = R\cdot i^{*\,2}_{\mathrm{q1}} = R\cdot(T^*_{em}/\kappa_{\mathrm{q1}})^2 = (2/9)\cdot(1/P_p^2)\cdot(R\cdot T^{*\,2}_{em}/\lambda^2_{M1})$ and each phase current is a sinusoidal function of θ.

However, the machine's mathematical model, written in the rotating reference frames as per (7), highlights that all the quadrature components i_{qh} of the current set $[i_{\mathrm{dq}}]$ actively influence T_{em}, and their contribution is proportional to the harmonic index h and to the corresponding flux magnitude λ_{Mh}. As a result, the system has more degrees of freedom which can be exploited to achieve certain optimization goals while guaranteeing the desired torque T^*_{em}.

Given that $[\kappa]$ is independent of θ, a constant torque can be obtained by simply using a constant $[i_{\mathrm{dq}}]$ set. With this choice, since each (i_{dh}, i_{qh}) subset is subject to a $h\theta$ rotation in the inverse transformations (6), all the phase currents i_k would be given as the superposition of sinusoidal components varying with $h\theta$. As a result, the simultaneous exploitation of different current components is equivalent to a harmonic injection into the phase currents.

An optimal strategy can be obtained by choosing the current vector $[i_{\mathrm{dq}}]$ capable of minimizing the machine's average power losses. Given (7)-(8), this approach can be formalized as the constrained optimization problem:

$$\begin{cases} \min\limits_{[i_{\mathrm{dq}}]\in\mathbb{R}^n}\left\{P\left([i_{\mathrm{dq}}]\right) = R\cdot I^2_{RMS} = R\cdot[i_{\mathrm{dq}}]^{\mathrm{T}}\cdot[\mathrm{H}]\cdot[i_{\mathrm{dq}}]\right\} \\ \text{subject to}\quad [\kappa]^{\mathrm{T}}\cdot[i_{\mathrm{dq}}] = T^*_{em} \end{cases} \tag{13}$$

where the current I_{RMS} represents an equivalent Root Mean Square (RMS) current for the whole machine; its minimization for a given reference torque can be interpreted as a Maximum-Torque-Per-Ampere (MTPA) strategy.

The problem (13) can be analytically solved by using the Lagrange multiplier method. The associated Lagrangian is:

$$\mathfrak{L}\left([i_{\mathrm{dq}}],\mu\right) = \frac{1}{2}\left([i_{\mathrm{dq}}]^{\mathrm{T}}\cdot[\mathrm{H}]\cdot[i_{\mathrm{dq}}]\right) + \mu\cdot\left(T^*_{em} - [\kappa]^{\mathrm{T}}\cdot[i_{\mathrm{dq}}]\right) \tag{14}$$

where the dependence on R has been neglected and μ is the multiplier associated to the equality constraint. By nullifying the gradient of $\mathfrak{L}$, the following linear system is obtained:

$$\begin{cases} [\mathrm{H}]\cdot[i^*_{\mathrm{dq}}] - \mu\cdot[\kappa] = [0_{9\times1}] \\ [\kappa]^{\mathrm{T}}\cdot[i^*_{\mathrm{dq}}] = T^*_{em} \end{cases} \tag{15}$$

Then, by solving (15) and recalling the explicit expressions of [H] and $[\kappa]$, the optimal current set is found:

$$\begin{aligned} [i^*_{\mathrm{dq}}] &= \frac{[\mathrm{H}]^{-1}\cdot[\kappa]}{[\kappa]^{\mathrm{T}}\cdot[\mathrm{H}]^{-1}\cdot[\kappa]}\cdot T^*_{em} = \\ &= \sqrt{\frac{2}{9}}\cdot\frac{T^*_{em}}{P_p}\cdot\frac{[0\ \ 5\lambda_{M1}\ \ 0\ \ 3\lambda_{M3}\ \ 0\ \ 25\lambda_{M5}\ \ 0\ \ 35\lambda_{M7}\ \ 0]^{\mathrm{T}}}{5\lambda^2_{M1} + 9\lambda^2_{M3} + 125\lambda^2_{M5} + 245\lambda^2_{M7}} \end{aligned} \tag{16}$$

As expected, all the direct components i_{dh}^{*} are kept at zero since they do not actively contribute to the torque, while the i_0^{*} component is set to zero in accordance with the constraint imposed by the isolated single neutral point configuration. All the quadrature components i_{qh}^{*} are proportional to T_{em}^{*} and their weight depends both on the magnitude of the corresponding PM's induced flux λ_{Mh} (via $[\kappa]$) and on their effect on the overall average power losses (via [H]).

The corresponding average power losses are:

$$P_{opt} = R\cdot\frac{[\kappa]^{\mathrm{T}}\cdot[\mathrm{H}]^{-1}\cdot[\mathrm{H}]\cdot[\mathrm{H}]^{-1}\cdot[\kappa]}{([\kappa]^{\mathrm{T}}\cdot[\mathrm{H}]^{-1}\cdot[\kappa])^{2}}\cdot(T_{em}^{*})^{2} = \\ = \frac{R\cdot(T_{em}^{*})^{2}}{[\kappa]^{\mathrm{T}}\cdot[\mathrm{H}]^{-1}\cdot[\kappa]} = \frac{2}{9}\cdot\frac{1}{P_p^{2}}\cdot\frac{5\cdot R\cdot(T_{em}^{*})^{2}}{5\lambda_{M1}^{2}+9\lambda_{M3}^{2}+125\lambda_{M5}^{2}+245\lambda_{M7}^{2}} \tag{17}$$

and, if compared with the exploitation of the fundamental component only, they guarantee a loss reduction of:

$$\eta_{opt} = \frac{P_{opt}}{P_{\mathrm{FUND}}} = \frac{\kappa_{\mathrm{q1}}^{2}/\mathrm{H}_{\mathrm{q1,q1}}}{[\kappa]^{\mathrm{T}}\cdot[\mathrm{H}]^{-1}\cdot[\kappa]} = \\ = \frac{5\lambda_{M1}^{2}}{5\lambda_{M1}^{2}+9\lambda_{M3}^{2}+125\lambda_{M5}^{2}+245\lambda_{M7}^{2}} \tag{18}$$

As is evident, $\eta_{opt} \le 1$, meaning that the proposed strategy can always guarantee better results than the exploitation of just the fundamental component. In particular, the higher the effect of the 3rd, the 5th and the 7th spatial harmonics in the PM's induced fluxes, the better the average stator loss reduction that can be achieved. Only when these components are absent (i.e. when $\lambda_{M3} = \lambda_{M5} = \lambda_{M7} = 0$), the result would be that $\eta_{opt} = 1$ and the strategy would be equivalent to a standard FOC, since only i_{q1} would be useful for torque development.

It is worth noticing that the proposed approach can be adapted to allow the exploitation of only a desired subset of harmonic components. As an example, the optimal third harmonic injection strategy, proposed in [21]-[22], can be obtained by nullifying the contributions of the 5th and 7th harmonics in the expression (16) by setting $\kappa_{\mathrm{q5}} = \kappa_{\mathrm{q7}} = 0$. Indeed, the corresponding current components $i_{\mathrm{q5}}^{*'}$ and $i_{\mathrm{q7}}^{*'}$ would be set to zero since (in the modified optimization problem) they would contribute to the average losses without developing any torque. In this case, the modified optimal current set would be:

$$[i_{\mathrm{dq}}^{*'}] = \sqrt{\frac{2}{9}}\frac{T_{em}^{*}}{P_p}\frac{[0\ \ 5\lambda_{M1}\ \ 0\ \ 3\lambda_{M3}\ \ 0\ \ 0\ \ 0\ \ 0\ \ 0]^{\mathrm{T}}}{5\lambda_{M1}^{2}+9\lambda_{M3}^{2}} \tag{19}$$

and the normalized power loss reduction would be:

$$\eta_{\mathrm{THI,opt}} = \frac{P_{\mathrm{THI,opt}}}{P_{\mathrm{FUND}}} = \frac{5\lambda_{M1}^{2}}{5\lambda_{M1}^{2}+9\lambda_{M3}^{2}} \tag{20}$$

This result is coherent with [21] and, as could be expected, $\eta_{opt} \le \eta_{THI,opt} \le 1$, meaning that the simultaneous exploitation of all the quadrature current components always gives better results than solely the third harmonic injection.

IV. Strategy Validation

The developed strategy has been numerically validated using the same machine analysed in [17,21,22], whose main parameters are summarized in Table I.

TABLE I NINE -PHASE MACHINE PARAMETERS

$P_p = 1$	$R = 31.3\ \Omega$	$L_{ls} = 84$ mH
$\lambda_{M1} = 385$ mWb	$\varphi_1 = 0°$	$L_1 = 147$ mH
$\lambda_{M3} = 119$ mWb	$\varphi_3 \cong 180°$	$L_3 = 92$ mH
$\lambda_{M5} = 38$ mWb	$\varphi_5 \cong 0°$	$L_5 = 88$ mH
$\lambda_{M7} = 7$ mWb	$\varphi_7 \cong 165°$	$L_7 = 87$ mH

A. Theoretical Optimal Results

The optimal synchronous current set $[i_{\mathrm{dq}}^{*}]$ is computed by substituting the numerical values of the flux magnitudes in (16). The resulting optimal phase current set $[i_{\mathrm{ph}}^{*}]$ is then found by applying the inverse transformation (6). The current waveforms and their harmonic spectra are depicted in Fig. 2, normalized by $I_{\mathrm{FUND}} = \sqrt{2/9}\,T_{em}^{*}/\kappa_{\mathrm{q1}}$, which is the peak current associated with the development of the same torque using only the fundamental component i_{q1}.

In agreement with the analytical results, only the 1st, 3rd, 5th and 7th harmonics of the spectra are present in the current Fourier decomposition. The waveforms of each three-phase $\{a,b,c\}$ set are identical and just mutually shifted by 120°.

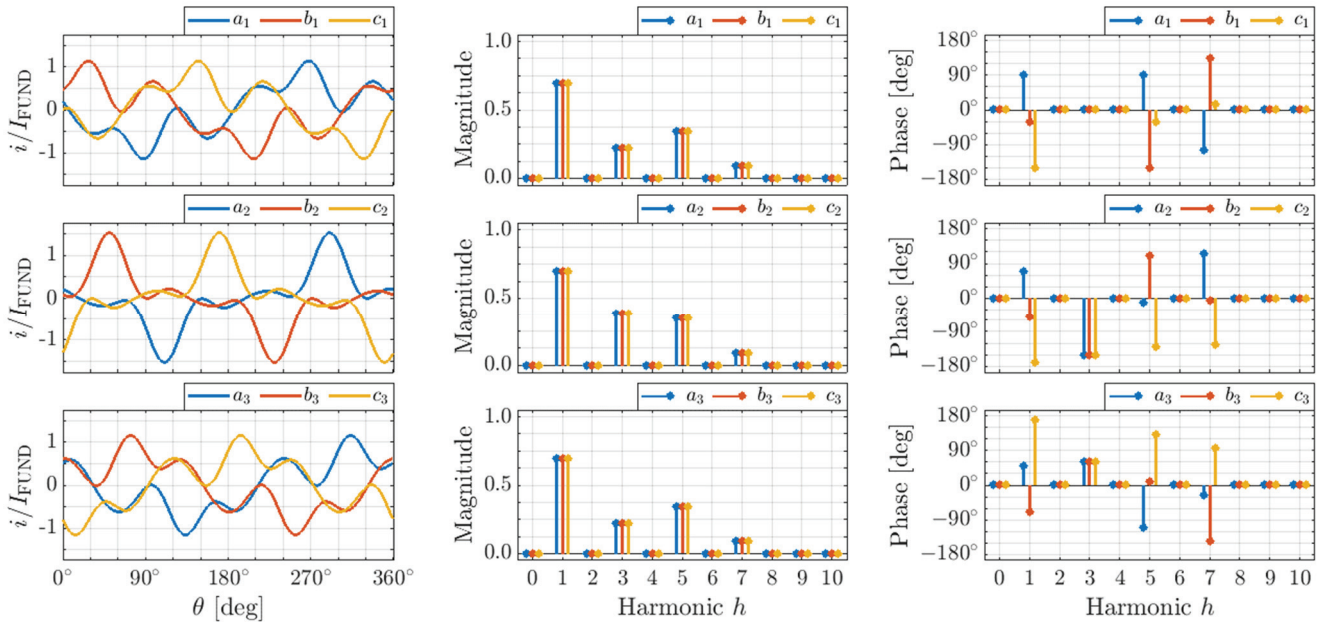

Fig. 2. Phase currents waveforms and harmonic spectra with the proposed optimal harmonic injection strategy.

Nevertheless, it can be immediately noticed that the three sets behave differently. Indeed, the third harmonic components are distributed unevenly among the machine's phases in order to guarantee that the sum of all the currents is zero. In particular, as can be seen from the harmonic spectra, the magnitude in the first and third set is equal, while the magnitude in the second set is $\sqrt{3}$ times higher. All the other harmonic components (related to i_{q1}, i_{q5} and i_{q7}) are equally distributed among all the phases.

Additionally, as a side effect of the harmonic injection, despite the reduction in their RMS value, the peak values of all the phase currents are higher than I_{FUND}, and the most affected set is $\{a_2,b_2,c_2\}$ where the peak is about 50% higher.

The unequal distribution of the currents also leads to an unequal distribution of the power losses. For the examined configuration it can be verified that the losses in the second set are about 36.5% of the total, while for the other two sets they are around 31.7% of the total. This behaviour is consistent with the analogous result obtained in [21-22], where only the third harmonic current injection was considered. In such a case both the first and the third set were responsible for the 31.3% of the total losses, while the second set was responsible for the remaining 37.4%.

However, in agreement with the optimization procedure, the overall power loss reduction with the proposed strategy (which is found as per (18)) is equal to $\eta_{opt} \approx 0.698$, leading to a power loss reduction of about 30%. This is significantly better than the power loss reduction obtained with the exploitation of the third harmonic only ($\eta_{THI,opt} \approx 0.853$, corresponding to a power loss reduction of about 15%).

B. *Simulation Results*

The strategy has been numerically tested in the Matlab/Simulink environment. During the whole simulation the machine is subject to a 2 Nm load torque and is kept at 600 rpm angular speed with a proper feedback control. The currents have been controlled by using the modified FOC algorithm described in [21-22], which includes an additional decoupling action in the d3-q3 subspace to neutralize the effect of the neutral point voltage v_{ON}.

A digital implementation of the controller has been executed with a 10 kHz sampling frequency, while the supplying inverter has been simulated with an average model to filter out the current ripple due to the pulse-width-modulation technique. Numerical results are depicted in Fig. 3 and show all the components of the $[i_{ph}]$ and $[i_{dq}]$ sets, the developed electromagnetic torque T_{em} and the stator power losses P, obtained by averaging the instantaneous power losses p in a moving time window of $T_0 = 100$ ms (one fundamental period) through the relation:

$$P(t) = \frac{1}{T_0} \cdot \int_{t-T_0}^{t} p(\tau)\,\mathrm{d}\tau = \frac{1}{T_0} \cdot \int_{t-T_0}^{t} \left[\sum_{k=1}^{9} R \cdot i_k^2(\tau) \right] \mathrm{d}\tau \qquad (21)$$

The simulation scenario is as follows. For the first 0.5 s ($[t_0,t_1]$ interval) the electromagnetic torque is developed by only exploiting the fundamental current harmonic (driven by i_{q1}), while keeping at zero all the other components of the synchronous current set $[i_{dq}]$. In the following 0.5 s time window ($[t_1,t_2]$ interval) the machine is controlled with the optimal third harmonic injection strategy presented in [21-22], therefore exploiting both i_{q1} and i_{q3} for the torque development. In the last 0.5 s ($[t_2,t_3]$ interval) the proposed strategy has been implemented, thus taking advantage of i_{q5} and i_{q7}, too.

By observing the current components in multiple synchronous frames (left column of Fig. 3) it can be immediately noted that all the direct axis components i_{dh} are effectively kept to zero by the feedback controller, while the zero sequence current i_0 is constrained to zero by the machine model (due to the single isolated neutral point configuration). The control of the quadrature axis current components i_{qh} is capable of quickly reacting to step changes of each reference and effectively stabilizes them to a desired constant value, thus highlighting the controller performance even in the case of fast current transients.

The optimal third harmonic injection strategy (applied after t_1) allows for a reduction of i_{q1}, while the proposed strategy (applied after t_2) makes it possible to reduce both i_{q1} and i_{q3} by increasing i_{q5} and i_{q7} accordingly.

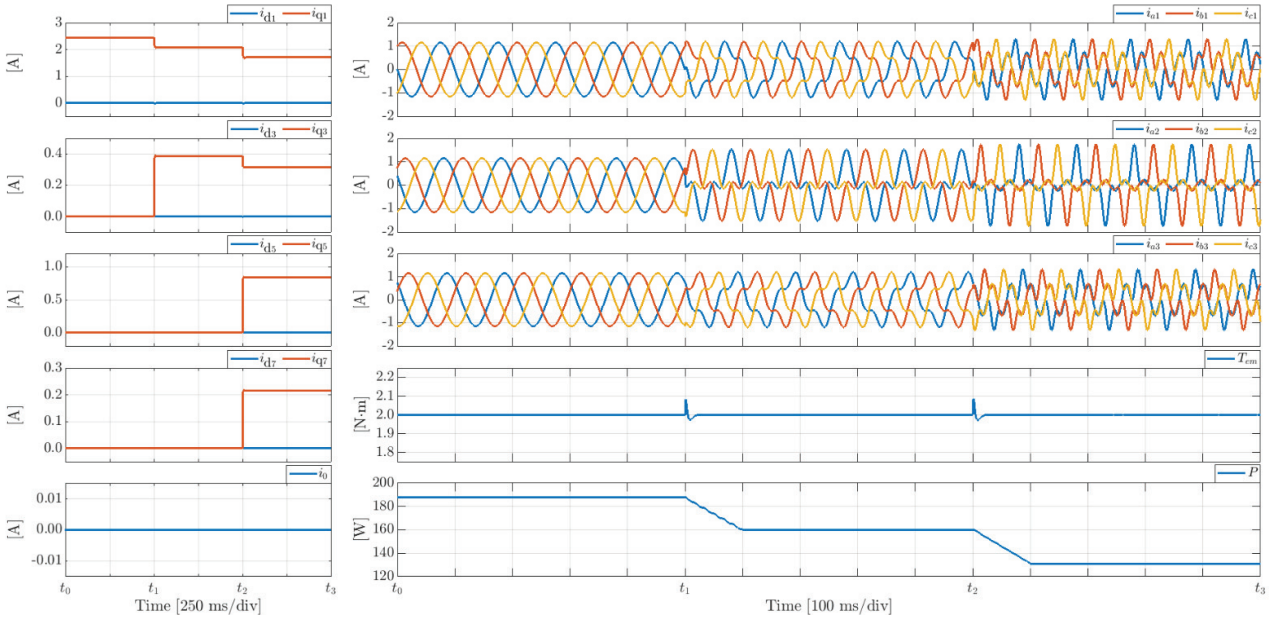

Fig. 3. Simulation results with different control strategies: $[t_0,t_1]$ Fundamental current component only; $[t_1,t_2]$ Optimal third harmonic current injection; $[t_2,t_3]$ Optimal multiple harmonic current injection.

The corresponding phase currents are depicted in the right column of Fig. 3. They are purely sinusoidal during the initial $[t_1,t_2]$ interval; in the $[t_1,t_2]$ time interval (with the optimal third harmonic injection) they follow the theoretical waveforms obtained in [21], while in the final $[t_2,t_3]$ interval their waveforms match the results depicted in Fig. 2.

As is evident, apart from a small transient deviation during the control strategy transitions, the electromagnetic torque T_{em} is always kept equal to the required 2 Nm, meaning that the equality constraint in the optimization problem (13) is met.

The stator average power losses P, with an initial value of about 188 W, are first decreased to 160 W with the optimal i_{q3} control, and then further reduced to about 131 W with the proposed optimal strategy, thus matching the $\eta_{THI,opt} \approx 0.853$ and $\eta_{opt} \approx 0.698$ values obtained with the theoretical analysis. The smooth decrease of the power loss waveform is due to the moving averaging procedure (18) and, indeed, takes just one fundamental period (100 ms).

V. Conclusions

The paper presented a strategy to optimally exploit multiple harmonic current injection for an asymmetrical nine-phase PMSM with non-sinusoidal back-EMF and a single isolated neutral point configuration.

By writing the machine's mathematical model in a multiple synchronous domain it has been possible to highlight that the electromagnetic torque development is given by the superposition of different quadrature current component contributions, each of which is related to a proper spatial harmonic of the magnetic flux density in the air-gap.

The simultaneous exploitation of all the available quadrature current components allows to meet a defined optimization goal. The approach has focused on the minimization of the average stator losses for a given reference torque. This choice represents an MTPA strategy or, equivalently, an optimal multiple harmonics injection in the machine's phase currents.

The solution has been found analytically by solving a quadratic programming problem with a linear equality constraint. The strategy can be easily adapted to exploit only a subset of the available harmonic components, while forcing the other terms to zero.

The total losses can be effectively reduced with respect to the sole exploitation of the fundamental current, but, in contrast to the symmetrical nine-phase machine configuration, they are not equally shared among all the phases.

The theoretical results have been validated through numerical analysis and simulations in the Matlab/Simulink environment. The proposed approach has successfully led to a significant improvement with respect to both the fundamental current component exploitation only and to the optimal third harmonic injection strategy developed previously.

References

[1] E. Levi, "Multiphase electric machines for variable-speed applications," *IEEE Trans. Ind. Electron.*, vol. 55, no. 5, pp. 1893-1909, 2008.

[2] E. Levi, F. Barrero and M. J. Duran, "Multiphase machines and drives – revisited," *IEEE Trans. Ind. Electron.*, vol. 63, pp. 429-432, 2016.

[3] E. Levi, R. Bojoi, F. Profumo, H. A. Toliyat and S. Williamson, "Multiphase induction motor drives - a technology status review," *IET Electr. Power Appl.*, vol. 1, no. 4, pp. 489-516, 2007.

[4] K. Wang, Z. Y. Gu, Z. Q. Zhu and Z. Z. Wu, "Optimum injected harmonics into magnet shape in multiphase surface-mounted PM machine for maximum output torque," *IEEE Trans. Ind. Electron.*, vol. 64, no. 6, pp. 4434-4443, 2017.

[5] K. Wang, "Effects of harmonics into magnet shape and current of dual three-phase permanent magnet machine on output torque capability," *IEEE Trans. Ind. Electron.*, vol. 65, no. 11, pp. 8758-8767, 2018.

[6] J. Wang, L. Zhou and R. Qu, "Harmonic current effect on torque density of a multiphase permanent magnet machine," *Int. Conf. Electric Mach. and Sys. ICEMS*, pp. 1-6, 2011.

[7] M. Farshadnia, M. A. Masood Cheema, A. Pouramin, R. Dutta and J. E. Fletcher, "Design of optimal winding configurations for symmetrical multiphase concentrated-wound surface-mount PMSMs to achieve maximum torque density under current harmonic injection," *IEEE Trans. Ind. Electron.*, vol. 65, no. 2, pp. 1751-1761, 2018.

[8] L. Parsa and H. A. Toliyat, "Five-phase permanent magnet motor drives," *IEEE Trans. Ind. Appl.*, vol. 41, no. 1, pp. 30-37, 2005.

[9] L. Parsa and H. A. Toliyat, "Five-phase permanent magnet motor drives for ship propulsion applications," *IEEE Electric Ship Tech. Symp. ESTS*, pp. 371-378, 2005.

[10] P. J. McCleer, J. M. Bailey and J. S. Lawler, "Five phase trapezoidal back emf PM synchronous machines and drives," *Eur. Power Electron. and Appl. Conf. EPE*, pp. 4.128-4.133, 1991.

[11] Z. Q. Zhu, K. Wang and G. Ombach, "Optimal magnet shaping with third order harmonic for maximum torque in SPM machines," 6*th IET Conf. on Power Electron., Mach. and Drives PEMD*, pp. 1-6, 2012.

[12] K. Wang, Z. Y. Gu, C. Liu and Z. Q. Zhu, "Design and analysis of a five-phase SPM machine considering third harmonic current injection," *IEEE Trans. Energy Conv.*, vol. 33, no. 3, pp. 1108-1117, 2018.

[13] B. Aslan and E. Semail, "New 5-phase concentrated winding machine with bi-harmonic rotor for automotive application," *Int. Conf. Electric Mach. ICEM*, pp. 2114-2119, 2014.

[14] Y. Sui, P. Zheng, Y. Fan and J. Zhao, "Research on the vector control strategy of five-phase PMSM based on third-harmonic current injection," *IEEE Int. Electric Mach. and Drives Conf. IEMDC*, pp. 1-8, 2017.

[15] Z. Y. Gu, K. Wang, Z. Q. Zhu, Z. Z. Wu, C. Liu and R. W. Cao, "Torque improvement in five-phase unequal tooth SPM machine by injecting third harmonic current," *IEEE Trans. Vech. Techn.*, vol. 67, 2018.

[16] J. Gong, H. Zahr, E. Semail, M. Trabelsi, B. Aslan and F. Scuiller, "Design considerations of five-phase machine with double p/3p polarity," *IEEE Trans. Energy Conv*, vol. 34, no. 1, pp. 12-24, 2019.

[17] M. Slunjski, M. Jones, E. Levi, "Analysis of a symmetrical nine-phase machine with highly non-sinusoidal back-EMF force," 44*th Ann. Conf. of IEEE Ind. Electron. Soc. IECON*, pp. 6229-6234, 2018.

[18] K. Wang, J. Y. Zhang, Z. Y. Gu, H. Y. Sun and Z. Q. Zhu, "Torque improvement of dual three-phase permanent magnet machine using zero sequence components," *IEEE Trans. Magnetics*, vol. 53, no. 11, 2017.

[19] K. Wang, Z. Q. Zhu, Y. Ren and G. Ombach, "Torque improvement of dual three-phase permanent-magnet machine with third-harmonic current injection," *IEEE Trans. Ind. Electron.*, vol. 62, no. 11, pp. 6833-6844, 2015.

[20] Y. Hu, Z. Q. Zhu, M. Odavic, "Torque capability enhancement of dual three-phase PMSM drive with fifth and seventh current harmonics injection," *IEEE Trans. Ind. Appl*., vol. 53, no. 5, pp. 4526-4535, 2017.

[21] A. Cervone, M. Slunjski, E. Levi and G. Brando, "Optimal third-harmonic current injection for an asymmetrical nine-phase PMSM with non-sinusoidal back-EMF" *45th Ann. Conf. of IEEE Ind. Electron. Soc. IECON*, pp. 6223-6228, 2019.

[22] A. Cervone, M. Slunjski, E. Levi and G. Brando, "Optimal third-harmonic current injection for asymmetrical multiphase PMSMs", *IEEE Trans. Ind. Electron.*, vol. 68, 2021, DOI: 10.1109/TIE.2020.2982099.